

August 3, 2016

Response to Comments

Comments are in black font and our responses are in *italicized font*.

Associate Editor

Dear Authors,

Even without looking in detail at the main manuscript, more work is needed. I would start with the Table and Figures. Normally these are self-explanatory or mostly, some of yours lack this. These are my suggestions for improvement.

Thank you very much for your helpful suggestions. We have revised the manuscript accordingly.

Table 1 I would not put the 14 sites in alphabetically order, but select a parameter relevant to the explaining the observations in your work, e.g. you could list them in order of low to high precipitation or temperature or the other way.

Based on the correlation in Fig. 3, we have re-ordered them according to latitude. Please see Table 1 for revision.

Fig 1. The placing of the locations and displayed parameters on the USA map is nice, but why do I need to look at them on a map? Is there more C up North more bound Fe-C, maybe indicate what it shows with a view arrows is it related to T or precipitation, see comment Table 1 maybe this is the parameter to list Table 1 under.

As similar as for Table 1, there is generally higher TC and TOC in soils with higher latitude. We feel it is good to keep them in the map. We revised the figure caption accordingly to emphasize the trend.

Fig 2 what relationship are shown, if the are there they are not obvious. If there are no relationship, why put in a figure at all.

Fig. 2A shows the contents of reactive iron and OC:Fe molar ratio. Fig. 2B shows the variations in OC:Fe, discussed in the manuscript. Fig. 2B was moved to the supplementary material.

Fig 3 Do we need all the show subfigures? I would prefer a selection of the most pertinent examples which link to the text, with the rest going to supplementary material.

Partial of Fig. 3 was moved to supplementary material.

Fig 4 This is very poor Figure, messy and unclear it gives a bad impression of overall standard of the manuscript, it lets your paper down.

This figure has been improved accordingly. The relationships between labile carbon/uncalibrated Fe-bound organic carbon and texture were kept. Relationship between Fe-bound organic carbon and texture was moved to supplementary material, as there is no significant correlation.

Fig 5 see comment Fig 3

We kept the spectra for aliphatic carbon in the manuscript, and moved other spectra to supplementary material.

Fig 6. A lot of information but no self-evident message from both Figures, please condense the information more and better.

This figure has been improved by keeping the ^{13}C for Fe-bound OC and non-Fe-bound OC in the manuscript, and moving other data to the supplementary material. Now, it clearly showed the enrichment of ^{13}C in Fe-bound OC.

1 Iron-Bound Organic Carbon in Forest Soils: Quantification 2 and Characterization

3 Qian Zhao¹, Simon R Poulson², Daniel Obrist³, Samira Sumaila^{4, 5}, James J.
4 Dynes⁴, Joyce M. McBeth^{4, 5}, Yu Yang^{1*}

5 [1] {Department of Civil and Environmental Engineering, University of Nevada, Reno, Nevada, 89557}

6 [2] {Department of Geological Sciences and Engineering, University of Nevada, Reno, Nevada, 89557}

7 [3] {Division of Atmospheric Sciences, Desert Research Institute, Reno, Nevada, 89512}

8 [4] {Canadian Light Source, 44 Innovation Blvd, Saskatoon, SK, S7N 2V3, Canada}

9 [5] {Department of Geological Sciences, University of Saskatchewan, Saskatoon, SK, S7N 5E2, Canada}

10 * Correspondence to: Y. Yang (yuy@unr.edu)

11 12 **ABSTRACT**

13 Iron oxide minerals play an important role in stabilizing organic carbon (OC) and regulating the
14 biogeochemical cycles of OC on the earth surface. To predict the fate of OC, it is essential to
15 understand the amount, spatial variability, and characteristics of Fe-bound OC in natural soils. In
16 this study, we investigated the concentrations and characteristics of Fe-bound OC in soils
17 collected from 14 forests in the United States, and determined the impact of ecogeographical
18 variables and soil physicochemical properties on the association of OC and Fe minerals. On
19 average, Fe-bound OC contributed 37.8% of total OC (TOC) in forest soils. Atomic ratios of
20 OC:Fe ranged from 0.56 to 17.7 with values of 1-10 for most samples, and the ratios indicate the
21 importance of both sorptive and incorporative interactions. The fraction of Fe-bound OC in TOC
22 ($f_{\text{Fe-OC}}$) was not related to the concentration of reactive Fe, which suggests that the importance of
23 association with Fe in OC accumulation was not governed by the concentration of reactive Fe.
24 Concentrations of Fe-bound OC and $f_{\text{Fe-OC}}$ increased with latitude and reached peak values at a
25 site with a mean annual temperature of 6.6 °C. Attenuated total reflectance-Fourier transform
26 infrared spectroscopy (ATR-FTIR) and near-edge X-ray absorption fine structure (NEXAFS)
27 analyses revealed that Fe-bound OC was less aliphatic than non-Fe-bound OC. Fe-bound OC

28 also was more enriched in ^{13}C compared to the non-Fe-bound OC, but C/N ratios did not differ
29 substantially. In summary, ^{13}C -enriched OC with less aliphatic carbon and more carboxylic
30 carbon was associated with Fe minerals in the soils, with values of $f_{\text{Fe-OC}}$ being controlled by
31 both sorptive and incorporative associations between Fe and OC. Overall, this study
32 demonstrates that Fe oxides play an important role in regulating the biogeochemical cycles of C
33 in forest soils, and uncovers the governing factors for the spatial variability and characteristics of
34 Fe-bound OC.

35

36 **1 Introduction**

37 Soil organic carbon (OC) in forests is a vital component of C biogeochemical cycles
38 (Eswaran et al., 1999). Global warming can potentially accelerate the decomposition of forest
39 soil OC, contributing to greenhouse gas emissions (Steffen et al., 1998). Alternatively, forest
40 soils can act as strong sinks for OC, if appropriate management is implemented, such as forest
41 harvesting and fire treatment (Eswaran et al., 1999; Johnson and Curtis, 2001). Understanding
42 the fate and stability of forest OC is important for evaluating and managing the global C cycle
43 under the framework of climate change.

44 Currently, there is an information gap concerning the stability and residence time of OC,
45 contributing to the problem that the residence time of OC (ranging from months to hundreds of
46 years) is a major source of uncertainty in modeling and prediction of C cycles (Schmidt et al.,
47 2011; Riley et al., 2014). Many concepts have been proposed to account for OC stabilization and
48 therefore residence times, including molecular recalcitrance, physical occlusion, and chemical
49 protection (Sollins et al., 1996; Krull et al., 2003; Baldock et al., 2004; Mayer et al., 2004;
50 Zimmerman et al., 2004; Schmidt et al., 2011). In general, the stability of OC is regulated by
51 biogeochemical reactions occurring at the interfaces between OC, minerals, and microorganisms,
52 and further knowledge about the mechanism for OC stabilization is critical for building up
53 process-based models to simulate and predict C cycles.

54 A number of lines of evidence suggest a key importance of iron oxide minerals in the
55 stabilization of OC (Kalbitz et al., 2005; Kaiser and Guggenberger, 2007; Wagai and Mayer,
56 2007). Iron oxides have a relatively high sorption capacity for OC, with sorption coefficients for
57 OC much higher than that of other metal oxides (Kaiser and Guggenberger, 2007; Chorover and

58 Amistadi, 2001). Wagai and Mayer (2007) reported Fe-bound OC concentrations in soils up to
59 22 mg g⁻¹ soil, contributing up to 40% of total OC (TOC) for most forest soils. Similarly,
60 Lalonde et al. (2012) found that Fe-bound OC contributed 22% of TOC in sediments. Studies
61 have shown that Fe minerals protect OC from degradation and inhibit mineralization of OC
62 (Baldock and Skjemstad, 2000; Kalbitz et al., 2005). There is, however, no systematic study on
63 the occurrence of Fe-bound OC across different forests and its governing factors.

64 The overall goals of this study were to investigate the spatial variability of Fe-bound OC
65 across forest soils, the factors that control Fe-bound OC concentrations, and the characteristics of
66 Fe-bound OC with respect to the physicochemical properties of soils. In this study, we first
67 quantified the concentration of Fe-bound OC across 14 forest soils in the United States and
68 analyzed the spatial distribution and influences of ecogeographical factors. Second, we
69 investigated the impact of soil physicochemical properties on the Fe-OC associations. Third, we
70 studied molecular characteristics of Fe-bound OC vs. non-Fe-bound OC, including how Fe-OC
71 association influenced the chemical properties of OC and the stable isotope composition. Hence,
72 this study provided a systematic evaluation for the Fe-bound OC in United States forests, the
73 influences of ecological factors on the occurrence of Fe-bound OC, and the effects of association
74 with Fe on the chemical properties of OC.

75

76 **2. Methods & Materials**

77 **2.1 Chemicals and materials**

78 Reagents used for Fe reduction experiments include sodium bicarbonate (NaHCO₃:
79 Sigma-Aldrich, St. Louis, MO, USA), trisodium citrate dihydrate (Na₃C₆H₅O₇•2H₂O: Acros
80 Organics, New Jersey, USA), and sodium dithionite (Na₂S₂O₄: Alfa Aesar, Ward Hill, MA,
81 USA). All chemicals used were analytical grade.

82

83 **2.2 Soil sample collection, primary characterization and pretreatment**

84 Soil samples were collected from 14 forest sites in the United States (Obrist et al., 2011,
85 2012, 2015). The abbreviations and the basic information for the sites are summarized in Table 1.
86 More detailed information on the sites and sampling protocols can be found in previous
87 publications (Obrist et al., 2011, 2012, 2015). Briefly, two replicate plots at each forest site were

88 sampled. During 2007-2009, top soils (0-20 cm) from all sites were collected using clean latex
89 gloves and stainless steel sampling equipment. All the samples were immediately transferred to
90 plastic freezer bags and kept on ice before transportation to the laboratory. Soil texture was
91 analyzed by an ASTM 152-type hydrometer at the Soil Forage and Water Analysis Laboratory at
92 Oklahoma State University (Obrist et al., 2011). The soil pH was measured by mixing soil
93 particle with deionized (DI) water in a solid/solution ratio of 1:1 (Kalra, 1995). Soil samples
94 used in the experiments in this study were ground to < 500 μm and freeze-dried after the removal
95 of roots and visible plant material and large particles (>2 mm) by dry sieving.

96

97 **Table 1**

98

99 **2.3 Total C (TC), TOC and stable C isotope analyses**

100 TC, TOC and stable C isotopic compositions of soil samples were analyzed using a
101 Eurovector elemental analyzer (Eurovector SPA, Milan, Italy) interfaced to a Micromass
102 IsoPrime stable isotope ratio mass spectrometer (Micromass UK Ltd., Manchester, UK).
103 Acetanilide (71.09 % C by weight) was used as a standard compound to establish a calibration
104 curve between mass of C and the m/z 44 response from the mass spectrometer. In this study, the
105 concentration of TC and TOC were expressed as weight %. Stable C isotope analyses were
106 performed after the method of Werner et al. (1999), with results reported in the usual delta
107 notation in units of ‰ vs. Vienna Pee Dee Belemnite (VPDB). For TOC analysis, soil samples
108 were acidified with 1 M HCl with the solution/solid ratio of 1 mL solution/0.5 g soil and heated
109 at 100°C for 1 hour. The treatment was repeated three times until there was no further
110 effervescence upon acid addition, after which the samples were dried and analyzed. All analyses
111 are based on standard curves with $R^2 > 0.99$. The detection limit for C is 0.2 mg g⁻¹ soil. The
112 average coefficient of variation for the analysis of C is 20.2%.

113

114 **2.4 Nitrogen (N) analysis**

115 The N concentration of each sample was analyzed using a Eurovector elemental analyzer.
116 Acetanilide (10.36 % N by weight) was used as a standard compound to establish a calibration
117 curve between mass of N and the response of the thermal conductivity detector in the elemental
118 analyzer. Total N and non-Fe-bound N concentrations were measured before and after a Fe

119 reduction release treatment for each sample. All analyses are based on standard curves with
120 $R^2 > 0.99$. The detection limit for N is 0.2 mg g⁻¹ soil. The average coefficient of variation for the
121 analysis of N is 20.5%.

122

123 **2.5 Analysis of Fe-bound OC**

124 The concentration of Fe-bound OC was quantified by an established Fe reduction release
125 method, commonly known as DCB extraction involving sodium dithionite, citrate and
126 bicarbonate (Mehra and Jackson, 1960; Wagai and Mayer, 2007; Lalonde et al., 2012). The DCB
127 extraction is assumed to extract most free Fe oxides (i.e. goethite, hematite, ferrihydrite and
128 others) existing in soils, but should not extract structural Fe in clay minerals (Mehra and Jackson,
129 1960; Wagai and Mayer et al., 2007; Lalonde et al., 2012). In this study, we followed the specific
130 protocol detailed in Lalonde et al. (2012). An aliquot (0.25 g) of soil was mixed with 15 mL of
131 buffer solution at pH 7 (containing 0.11 M bicarbonate and 0.27 M trisodium citrate), and then
132 heated to 80°C in a water bath. The reducing agent sodium dithionite was added to the samples
133 with final concentration of 0.1 M, and maintained at 80°C for 15 min. The samples were then
134 centrifuged at 10,000 rpm for 10 min, the supernatant was removed, and the residual particles
135 were rinsed using 5 mL of DI water. The rinse/centrifuge process was performed three times.
136 The residual particles were freeze-dried and analyzed for TC and TOC concentrations and $\delta^{13}\text{C}$
137 composition. The mass of residual particles was used to calculate the OC concentration
138 associated with non-Fe minerals.

139 The background release of OC during the heating process was measured following the
140 method in Lalonde et al. (2012), where sodium citrate and dithionite were replaced by sodium
141 chloride with the same ionic strength. An aliquot (0.25 g) of dry soil was mixed with 15 mL of
142 1.6 M NaCl and 0.11 M NaHCO₃, and heated to 80°C. Then 0.22 g of NaCl was added, and the
143 solution was maintained at 80°C for 15 min. The samples were then centrifuged at 10,000 rpm
144 and rinsed three times, and freeze-dried before analysis. The mass of residual particles was used
145 to calculate the concentration of OC released by heating to 80°C. In preliminary experiments, we
146 found that the solution pH increased rapidly during the heating-extraction process with
147 bicarbonate and sodium chloride only, and the increased pH values facilitated the release of
148 additional OC. Hence, we used a lower initial pH of 6 to compensate for the shift to higher pH
149 during heating. To validate the measurement for the concentration of OC released during heating,

150 we also tested the release of OC using a phosphate buffer (same ionic strength) in lieu of the
151 bicarbonate buffer, which can maintain a pH of 7 during heating. Our results showed that the
152 concentration of OC released was similar for both the bicarbonate and phosphate buffer
153 extraction reactions (Supplementary Material, Fig. S1).

154

155 **2.6 Quantification of reactive Fe**

156 The concentration of reactive Fe in soils was determined by analyzing the Fe released
157 during the DCB reduction process. After the reduction treatment, the supernatant of each sample
158 was filtered using a 0.2 μm syringe filter (cellulose acetate), and analyzed for Fe concentration
159 by inductively coupled plasma - atomic emission spectroscopy (Varian-Vista AX CCD, Palo
160 Alto, CA, USA) at an optical absorption wavelength of 259.9 nm. All analyses are based on
161 standard curves with $R^2 > 0.99$. The detection limit for Fe is 0.04 mg g^{-1} soil. The average
162 coefficient of variation for the analysis of Fe is 25.8%.

163

164 **2.7 Attenuated total reflectance-Fourier transform infrared spectroscopy (ATR-FTIR)**

165 ATR-FTIR analysis to characterize the molecular composition of OC was performed for
166 original soil samples and residual soils after DCB extraction using a Thermo Scientific Nicolet
167 6700 FTIR (Waltham, MA). Dry soil samples were placed directly on the crystal and forced to
168 contact well with the crystal. Spectra were acquired at the resolution of 4 cm^{-1} based on 100
169 scans. Data collection and baseline correction were accomplished using OMNIC software
170 version 8.3.103.

171

172 **2.8 Near-edge X-ray absorption fine structure (NEXAFS) analysis**

173 For further characterization of chemical structure of OM, carbon (1s) K-edge NEXAFS
174 analyses were performed for select soil samples, i.e. for soils with the highest and lowest values
175 of the fraction of Fe-bound OC to TOC. The soil particles were suspended in DI water and
176 deposited on an Au-coated silicon wafer attached to a Cu sample holder. Before analysis,
177 samples were dried in a vacuum desiccator. The X-ray-based experiments were performed on the
178 Spherical Grating Monochromator (SGM) beamline at the Canadian Light Source (Saskatoon,
179 Canada) (Regier et al., 2007). The energy scale was calibrated using citric acid (absorption at
180 288.6 eV). Major technical parameters and set-up for the beamline include: X-ray energy ranges

181 250-2000 eV; 45 mm planer undulator; 1000 $\mu\text{m}\times 100\ \mu\text{m}$ spot size; silicon drift detectors (SDD);
182 a titanium filter before the sample; entrance and exit slit gaps of 249.9 μm and 25 μm (Gillespie
183 et al., 2015). Carbon 1s spectra were acquired by slew scans from 270 to 320 eV at 20 s dwell
184 time and 20 scans per sample on a new spot. For data normalization, I_0 was collected by
185 measuring the scatter of the incident beam from a freshly Au-coated Si wafer using SDD.
186 Before the I_0 normalization, the pre-edge baseline was adjusted to near zero to remove the scatter
187 in the sample data (Gillespie et al., 2015).

188 **3. Results and Discussion**

189 **3.1 Concentration of Fe-bound OC**

190 This study covered five major forest types in North America, including Spruce-Fir, Pine,
191 Oak, Chaparral, and Maple-beech-birch forests distributed between 29° and 47° N. For the 14
192 forest soils, TC concentrations ranged between 1.5 \pm 0.1 and 8.3 \pm 2.1% (all percentages given are
193 weight-based), and TOC concentrations ranged between 1.3 \pm 0.3 and 6.2 \pm 2.9%, which are
194 comparable to values previously reported for North American forest soils (Wagai and Mayer,
195 2007; Wilson et al., 2013). Bicarbonate extraction-calibrated Fe-bound OC concentrations
196 ranged from 0.3 to 1.9%, with the fraction of Fe-bound OC to TOC ($f_{\text{Fe-OC}}$) averaging 37.8 \pm 20.0%
197 (Fig. 1, Supplementary Material, Table S1). Forest HL (Maine) had the highest $f_{\text{Fe-OC}}$ of 57.8%,
198 while forests GS (Florida) and OR (Tennessee) had $f_{\text{Fe-OC}}$ values below detection limits (i.e.,
199 below 0.6%). Based on an estimate that 1502 Pg (Pg=1 \times 10¹⁵ g) of TOC is stored in terrestrial
200 soils (Scharlemann, et al., 2014), scaling up these results to a global estimate would yield
201 538.5 \pm 271.5 Pg of Fe-bound OC residing in terrestrial soils.

202

203 **Fig. 1**

204

205 **3.2 Fe-OC association**

206 The values of $f_{\text{Fe-OC}}$ were influenced not only by the concentration of reactive Fe, but also
207 by the type of association between Fe and OC. In this study, the concentration of reactive Fe in
208 forest soils ranged from 0.1 mg g⁻¹ to 19.3 mg g⁻¹, which is low compared to values of reactive
209 Fe of up to 180 mg g⁻¹ reported previously (Wagai and Mayer, 2007; Wagai et al., 2013) (Fig. 2).
210 A Mollisol in forest site MS (California) had the highest concentration of reactive Fe, while a

211 Spodosol in forest site GS (Florida) had the lowest reactive Fe concentration. There was no
212 significant correlation between $f_{\text{Fe-OC}}$ and the concentration of reactive Fe (Pearson Correlation
213 Coefficient $r=-0.418$, $p=0.137$, **Supplementary Material, Fig. S2**). This suggests that the
214 proportion of Fe-bound OC is not strongly controlled by the reactive Fe concentration.

215

216 **Fig. 2.**

217

218 The OC:Fe molar ratio ranged from 0.56 to 17.7 for all 14 soils, with a value between 1
219 and 10 for 10 soils (**Fig. 2**). Previous studies have suggested that the OC:Fe molar ratio can be
220 used as an indicator for the type of association between Fe oxides and OC, with lower values
221 indicating sorptive interactions while higher values indicate incorporation of OC within Fe
222 oxides (Wagai et al., 2007; Guggenberger and Kaiser, 2003). The highest sorption capacity
223 measured for OC onto Fe oxide corresponds to an OC:Fe molar ratio = 1.0 (Kaiser and
224 Guggenberger, 2006), but by incorporation and co-precipitation of Fe oxide OC:Fe molar ratio
225 can reach much higher values (Guggenberger and Kaiser, 2003). With OC:Fe molar ratios
226 generally between 1-10 for about two thirds of the forest soils in this study, we propose that
227 incorporation of OC into Fe oxides plays a major role in the accumulation of Fe-bound OC
228 exceeding sorption by at least a factor of 1 to almost 20 (Wagai and Mayer, 2007; Lalonde, 2012).
229 However, for the HT (Michigan), HL (Maine) and TKF (California) forest soils, the OC:Fe
230 molar ratios were even higher than 10 with a maximum value of 17.8 (**Fig. 2**), implying that
231 incorporation of OC into Fe oxides dominated at these sites. Similar to $f_{\text{Fe-OC}}$, OC:Fe ratios were
232 not related to the concentration of reactive Fe and showed large variation for soils with similar
233 concentration of total reactive Fe (**Supplementary Material, Fig. S2**). This further indicates that
234 the type of interactions between OC and Fe was not governed by the amount of Fe. The OC:Fe
235 ratio is potentially regulated by the mineral phases of Fe, as poorly-crystalline Fe oxides have a
236 higher capacity to bind with OC than crystalline Fe minerals (Eusterhues et al., 2014). When
237 sorption dominates the interactions between OC and Fe, OC:Fe can also be influenced greatly by
238 the particle size and surface area of Fe oxides (Gu et al., 1995). Further investigations are needed
239 to determine the factors that control the OC:Fe ratio, and also $f_{\text{Fe-OC}}$ values for soils. Nevertheless,
240 the lack of (or poor) relationship shown here between the concentration of Fe-bound OC and Fe

241 concentrations demonstrates the limitations associated with predicting and modeling the behavior
242 of C in forest soils based on the Fe concentrations in soils alone.

243

244 **3.3 Spatial variance and ecogeographical factors**

245 We analyzed the influences of ecogeographical factors on the occurrence of Fe-bound OC in
246 forest soils (Fig. 3, **Supplementary Material, Fig. S3, Fig. S4**). There was a significant correlation
247 between the TOC concentration and latitude (Pearson correlation coefficient $r=0.619$, $p=0.018$),
248 a pattern commonly observed due to lower microbial activity and turnover rates of C at higher,
249 colder latitudes (Davidson and Janssens, 2006). The concentration of reactive Fe, if excluding
250 soil MS in California, was also significantly related to latitude ($r=0.824$, $p=0.001$). Both
251 concentrations of Fe-bound OC and $f_{\text{Fe-OC}}$ were also correlated with latitude ($r=0.523$, $p=0.053$;
252 $r=0.525$, $p=0.054$). Among our samples, the soil in forest HL in Maine, one of the three
253 northern-most site with latitude of 45° , had the highest $f_{\text{Fe-OC}}$ of 57.8%. In forest GS in Florida
254 with lowest latitude of 29.7° , the $f_{\text{Fe-OC}}$ was below detection limits, possibly due to the low
255 concentration of reactive Fe (0.08 mg g^{-1}). Hence, increase in latitude both increased
256 concentrations of TOC in soil as well concentrations of Fe-bound OC, suggesting increased
257 interactions between Fe oxide and OC at higher latitudes. There were no clear trends in TOC or
258 Fe-OC interactions with longitude. For elevation, we separated two groups of samples, with one
259 group located below 1000 m (asl) and the other group above (mainly around 2000 and 4000 asl).
260 Concentrations of TOC and Fe-bound OC, however, were not significantly different between the
261 two groups. There were no clear trends with precipitation either, although others have reported
262 positive relationships between mean annual precipitation and soil TOC concentration at a global
263 scale (Amundson, 2001). The concentration of Fe-bound OC and $f_{\text{Fe-OC}}$ reached peak value with
264 mean annual temperatures at 6.6°C , with lower values both at higher and lower temperatures.
265 Temperature dependence of Fe-bound OC can be regulated by effects of temperature on the
266 mineral phase of Fe oxides and OC dynamics. Given that ferrihydrite can incorporate more OC
267 than other crystalline Fe oxides, an increase in temperature favors the transformation of
268 ferrihydrite to other crystalline iron oxides (Gnanaprakash et al., 2007; Zhao et al., 1994).
269 However, an increase in temperature can also accelerate weathering of other minerals, and
270 increased release of silicon can slow the transformation of ferrihydrite (Cornell et al., 1987;
271 White and Blum, 1995). However, there is also evidence that temperature can affect the chemical

272 composition of soil OC substantially (Conant et al., 2011). For example, increased temperature
273 decreased the content of oxidized functional groups, such as saccharides, which would
274 consequently inhibit the interactions between OC and Fe oxides (Amelung et al., 1997). The
275 overall pattern can result from combined effects of temperature on Fe mineral phase and OC
276 transformation. Further investigations are required to elucidate the mechanism more accurately.
277 Finally, the study covered 7 major soil orders, i.e. Alfisols (sample number n=3), Spodosols
278 (n=4), Mollisols (n=1), Inceptisols (n=2), Entisols (n=2), Gelisols (n=1), and Ultisols (n=1).
279 Although there are limited replications in many of these soil orders, the highest concentration of
280 Fe-bound OC were observed in Spodosols. Regarding $f_{\text{Fe-OC}}$, the highest values were also found
281 in Spodosols, possibly indicating a particular importance of Fe-bound OC in this soil type which
282 occupies 3.5% of US land areas and 4% of global ice-free land (Soil Survey Staff, 1999).
283 However, due to the limited number of samples for each soil order, these findings warrant further
284 confirmation.

285

286 **Fig. 3**

287

288 **3.4 Impact of soil physicochemical properties on Fe-OC association**

289 Soil texture can potentially influence the accumulation of Fe-bound OC. Figure 4
290 demonstrates that the fraction of non-calibrated Fe-bound OC showed a significant positive
291 correlation with the fraction of sand ($r=0.72$, $p<0.001$), and negative correlations with the
292 fraction of silt ($r=-0.697$, $p<0.001$) and clay ($r=-0.616$, $p<0.001$). There were similar
293 correlations between labile OC and the fractions of sand ($r=0.57$, $p=0.033$), silt ($r=-0.51$,
294 $p=0.062$) and clay ($r=-0.638$, $p=0.014$). However, the calibrated Fe-bound OC had no significant
295 correlation with any of the texture fractions (Supplementary Material, Fig. S5). These
296 correlations indicate that the labile OC was mainly associated with the sand component of forest
297 soils, but that the soil texture did not affect the Fe-bound OC. There is debate on the relative
298 roles of sand, clay and silt in the stabilization of OC in soil (Percival et al., 2000; Six et al., 2002;
299 Eusterhues et al., 2005; Vogel et al., 2014). Eusterhues et al. (2005) found a relationship between
300 the resistance of organic matter to oxidative degradation and the clay concentration in soils,
301 suggesting the importance of clay minerals in the stabilization and accumulation of soil OC.
302 Reduced chemical potential of soil organic matter in small pores of clay-rich soils also limits

303 microbial degradation and enhance its stabilization (Riedel and Weber, 2016). In contrast,
304 Percival et al. (2000) found that the clay mineral fraction explained little of the variation in the
305 accumulation of OC across a range of soil types in New Zealand. Vogel et al. (2014) found that
306 less than 20% of clay mineral surfaces were covered by the sorption of OC, indicating that a
307 limited proportion of clay mineral surface contributed towards the stabilization of OC. Our
308 results suggest that the Fe oxide-mediated stabilization of OC was not related to the
309 size/aggregation-based process, although the labile carbon concentrations increased with the
310 fraction of sand in the soils.

311

312 **Fig. 4**

313

314 The Fe-OC association can also be influenced by the soil pH, which affects the mineral
315 phases of Fe oxides and their surface charge, and their interactions with OC. For our soil samples,
316 the soil pH ranged from 4.1 to 6.3, similar to measurements by Wagai and Mayer (2007) for
317 North America soils. There was no significant correlation between the $f_{\text{Fe-OC}}$ and soil pH, e.g. the
318 HL (Maine) soil with pH of 4.4 had the highest $f_{\text{Fe-OC}}$ of 57.8%, while the TS(II) (Washington)
319 soil with a similar pH of 4.5 only had a $f_{\text{Fe-OC}}$ of 7.4%. For soils with pH ranging from 4.9 to 5.8,
320 $f_{\text{Fe-OC}}$ did not change correspondingly. Contrastingly, values of OC:Fe molar ratios were
321 significantly influenced by the soil pH; except for one outlier sample of TS(II) (Washington)
322 soil, there was a significant negative correlation between the OC:Fe molar ratio and soil pH ($r=-$
323 0.477 , $p=0.09$) (Supplementary Material, Fig. S6). This may be due to the lower pH values
324 favoring the complexation and precipitation of Fe with OC, while higher pH favors sorptive
325 interactions between Fe minerals and OC (Tipping et al., 2002). If comparing samples with
326 similar pH, the soils with higher TOC had higher OC:Fe molar ratios, e.g. the GS soil (TOC =
327 1.1%) with pH of 4.7 had an OC:Fe molar ratio = 8.5, while the HT (Michigan) soil (TOC =
328 3.0%) with similar pH of 4.7 had an OC:Fe molar ratio = 17.1. This was consistent with
329 Schwertmann et al. (1986), who found that the major form of Fe would change from FeO_x to
330 complexes with OC when there is higher OC supply.

331

332 **3.5 Molecular characteristics of Fe-bound OC**

333 The chemical composition of Fe-bound OC can be substantially different from non-Fe-
334 bound OC (Adhikari and Yang, 2015) with broad implications on the C biogeochemical cycles,
335 although such differences so far have received limited attention. We analyzed the difference in
336 chemical composition of Fe-bound OC compared to non-Fe-bound OC using ATR-FTIR
337 analysis (Fig. 5, **Supplementary Material, Fig. S7**). Overall, there were limited fingerprint peaks
338 for OC, because of the low concentration of TOC and technical challenge for analyzing whole
339 soil particles with FTIR (Calderon et al., 2011; Simonetti et al., 2012). Reeves (2012)
340 demonstrated that FTIR analysis of mineral soils in the ranges of 1600-1750 and 2800-3000 cm^{-1}
341 only can be used to study OC. Peaks in the range of 500-1200 cm^{-1} indicate the presence of clay
342 or other Fe/Al minerals (**Supplementary Material, Fig. S7**) (Madejova, 2003; Harsh et al., 2002;
343 Parikh et al., 2014), such as kaolinite or montmorillonite at 850-1200 cm^{-1} (Madejova, 2003).
344 Absorption at 850-1200 cm^{-1} can also be due to the presence of polysaccharides, but definitive
345 identification of polysaccharides is not possible in the presence of minerals (Senesi et al., 2003;
346 Tandy et al., 2010). The spectra in the range of 1600-1750 cm^{-1} normally contain fingerprint
347 peaks for functional groups of amides, carboxylates and aromatics (Parikh et al., 2014), but we
348 did not detect any significant peaks in this range. In the range of 2800-3000 cm^{-1} , there were no
349 significant peaks for the original soil samples, but after Fe extraction we detected significant
350 peaks at 2850 and 2930 cm^{-1} , which are characteristic for the presence of aliphatic carbon. The
351 substantial differences in spectra before and after Fe extraction indicate that aliphatic OC was
352 enriched in the residual soils after extraction. Other functional groups, such as aromatic carbon
353 and hydrophilic functional groups, were more strongly associated with Fe minerals and removed
354 during the Fe extraction, as hydrophilic functional groups can form inner-sphere coordination
355 complexation with iron oxides, and aromatic carbon has electron donor-acceptor interactions
356 with iron oxides (Gu et al., 1995; Axe and Persson, 2001). This result was consistent with a
357 previous study using ultra-high resolution mass spectrometry, showing the release of more
358 aromatic carbon during the reductive dissolution of Fe oxides (Riedel et al., 2014). Analysis for
359 the chemical nature of Fe-bound OC can be influenced by the potential reaction of natural
360 organic matter with dithionite, which was not noticed in previous studies (Lalonde et al., 2012;
361 Wagai and Mayer, 2007). The most likely reaction between dithionite and organic matter is the
362 reduction of oxidized organic functional groups. Our recent study showed that dithionite could
363 reduce quinone groups in natural organic matter (Adhikari et al., 2016). Most likely, other major

364 functional groups, such as carboxylic and carbonyl functional groups, cannot be reduced by
365 dithionite based on their reduction potentials (Bar-Even et al., 2012; Mayhew et al., 1978).
366 Further investigations are needed to elaborate the detailed influences of dithionite reduction on
367 the molecular properties of organic matter.

368

369 **Fig. 5**

370

371 Furthermore, we analyzed the C 1s NEXAFS spectra of two original, non-extracted soils
372 with the highest and lowest values of $f_{\text{Fe-OC}}$, i.e. HL (Maine) ($f_{\text{Fe-OC}}=57.8\%$) and OR (Tennessee)
373 ($f_{\text{Fe-OC}}$ non-detectable) (Supplementary Material, Fig. S8). Three major fingerprint peaks were
374 detected for both soils, including peaks at 285.3, 287.0 and 288.7 eV, which are corresponding to
375 aromatic carbon, aliphatic carbon and carboxylic carbon, respectively (Schumacher et al., 2005;
376 Solomon et al., 2005; Lehmann et al., 2008). The OR (Tennessee) soil had a more substantial
377 signal at 287.0 eV than the HL (Maine) soil, indicating a higher aliphatic carbon concentration in
378 the OR (Tennessee) soil compared to the HL (Maine) soil. Ratio of carboxylic carbon to
379 aromatic carbon (peak height) was 3.8 for HL (Maine) and 1.0 for OR (Tennessee), suggesting
380 that the HL (Maine) soil with higher $f_{\text{Fe-OC}}$ has relatively more carboxylic carbon compared to
381 aromatic carbon. Hence, the C1s NEXAFS spectra suggest that the soil with the higher $f_{\text{Fe-OC}}$ has
382 higher concentration of carboxylic C, while the soil with the lower $f_{\text{Fe-OC}}$ value has a higher
383 aliphatic C concentration. This result is consistent with the comparison of ATR-FTIR spectra in
384 soils before and after Fe extraction, providing evidence that Fe oxides are mainly associated with
385 more hydrophilic and carboxylic carbon, while non-Fe-bound OC was more aliphatic.

386

387 To further investigate the relationships between soil OC and Fe minerals, we analyzed the
388 stable C isotopic compositions ($\delta^{13}\text{C}$) of Fe-bound vs. non-Fe-bound OC (i.e., the residual OC
389 after DCB extraction). The $\delta^{13}\text{C}$ for original soil samples ranged from -24.5% to -27.5% , and
390 the values for non-Fe-bound OC were -25.1% to -28.0% . The $\delta^{13}\text{C}$ for Fe-bound OC was
391 calculated by combined isotope-mass balance (equation (1))

$$392 \delta^{13}\text{C}_{\text{TOC}} \times \text{TOC} = \delta^{13}\text{C}_{\text{labile}} \times \text{OC}_{\text{labile}} + \delta^{13}\text{C}'_{\text{Fe-OC}} \times \text{OC}'_{\text{Fe}} + \delta^{13}\text{C}_{\text{non-Fe-OC}} \times \text{OC}_{\text{non-Fe}} \quad (1)$$

393 where TOC is the concentration of total organic carbon, $\text{OC}_{\text{labile}}$ is the concentration of labile OC
394 (extractable by bicarbonate buffer), $\text{OC}_{\text{non-Fe}}$ is the concentration of non-Fe-bound OC (residual

395 OC after Fe extraction), and OC'_{Fe} is the concentration of Fe-bound OC (excluded the labile OC);
 396 $\delta^{13}C_{TOC}$ is $\delta^{13}C$ for bulk OC, $\delta^{13}C_{labile}$ is $\delta^{13}C$ for labile OC, $\delta^{13}C'_{Fe-OC}$ is $\delta^{13}C$ for Fe-bound OC,
 397 $\delta^{13}C_{non-Fe-OC}$ is $\delta^{13}C$ for non-Fe-bound OC. However, it is difficult to directly resolve the $\delta^{13}C_{labile}$
 398 and $\delta^{13}C'_{Fe-OC}$ using this equation. We simplified it to equation (2):

$$399 \quad \delta^{13}C_{Fe-OC} = \frac{(\delta^{13}C_{TOC} \times TOC - \delta^{13}C_{non-Fe-OC} \times OC_{non-Fe})}{OC_{Fe}} \quad (2)$$

400 where $\delta^{13}C_{Fe-OC}$ is $\delta^{13}C$ for Fe-bound OC (including the labile OC), $\delta^{13}C_{TOC}$ is $\delta^{13}C$ for bulk OC,
 401 $\delta^{13}C_{non-Fe-OC}$ is $\delta^{13}C$ for non-Fe-bound OC, TOC is the concentration of total organic carbon,
 402 OC_{non-Fe} is the concentration of non-Fe-bound OC, and OC_{Fe} is the concentration of Fe-bound
 403 OC. The $\delta^{13}C$ for Fe-bound OC was heaviest for the TKF (California) soil with a value of –
 404 23.0‰, and the lightest for the GS (Florida) forest at –27.0‰. Across all study sites, Fe-bound
 405 OC was relatively enriched in ^{13}C (1.5 ± 1.2 ‰ heavier) compared to the non-Fe-bound OC.
 406 However, there is also a contribution of labile OC to the Fe-bound OC, where labile OC is the
 407 OC extracted during the dithionite-absent extraction described earlier). The $\delta^{13}C$ value for labile
 408 OC can be calculated using equation (3):

$$409 \quad \delta^{13}C_{labile} = \frac{(\delta^{13}C_{TOC} \times TOC - \delta^{13}C_{non-labile} \times OC_{non-labile})}{OC_{labile}} \quad (3)$$

410 where $\delta^{13}C_{labile}$ is $\delta^{13}C$ for labile OC, $\delta^{13}C_{TOC}$ is $\delta^{13}C$ for bulk OC, $\delta^{13}C_{non-labile}$ is $\delta^{13}C$ for non-
 411 labile OC, $OC_{non-labile}$ is the concentration of non-labile OC, and OC_{labile} is the concentration of
 412 labile OC. Calculated values of $\delta^{13}C_{labile}$ range from -23.4‰ to -30.3‰, and were lighter than the
 413 values for $\delta^{13}C_{Fe-OC}$. Although it is not reliable to quantitatively calculate the $\delta^{13}C$ for Fe-bound
 414 OC subtracting the influences of labile OC, these results indicate that the true value for $\delta^{13}C_{Fe-OC}$
 415 should be even somewhat heavier than the results presented in Fig. 6 **and Supplementary**
 416 **Material, Fig. S9**.

417 Our results demonstrate that Fe-bound OC was enriched in ^{13}C compared to the non-Fe-
 418 bound OC in forest soils, which is consistent with results for sediments, where Fe-bound OC was
 419 1.7 ± 2.8 ‰ heavier than non-Fe-bound OC (Lalonde et al., 2012) (Fig. 6A). Previous studies
 420 showed that ^{13}C -enriched organic matter in sediments was enriched with O and N (due to the
 421 presence of compounds such as proteins and carbohydrate groups), while the microbial biomass-
 422 derived lipid fraction was relatively ^{13}C -depleted (Wang et al., 1998; Zelles et al., 1992).
 423 Similarly, compound-specific isotopic analyses have shown that oxygen- and nitrogen-rich
 424 constituents, such as cellulose, hemi-cellulose and amino acids, are ^{13}C -enriched compared to

425 hydrocarbons (Glaser, 2005), and these ^{13}C -enriched oxygen- and nitrogen-rich compounds can
426 associate with Fe oxide extensively through inner-sphere coordination interactions (Parikh et al.,
427 2014). The value of $\Delta^{13}\text{C}_{\text{FeOC-nonFeOC}} = (\delta^{13}\text{C}_{\text{Fe-OC}} - \delta^{13}\text{C}_{\text{non-Fe-OC}})$ (difference in $\delta^{13}\text{C}$ for Fe-bound
428 OC and non-Fe-bound OC) was inversely correlated with the molar ratio of OC:Fe ($r=-0.53$,
429 $p=0.05$, Fig. 6B). These relationships suggest that the enrichment in ^{13}C was to some degree
430 related to the OC:Fe ratio. As discussed previously (section 3.2), lower OC:Fe ratios indicate an
431 increased contribution from sorptive interactions of OC with Fe minerals as compared to
432 incorporation of OC within iron oxides and OC, and these sorptive interactions between oxygen-
433 and nitrogen-rich organic compounds and Fe oxide results in the enrichment of ^{13}C of Fe-bound
434 OC vs. non-Fe-bound OC. Previous studies have attributed the stability of relatively labile and
435 reactive compounds, such as amino acids and sugars, to their interactions with minerals (Schmidt
436 et al., 2011), and our results demonstrated the importance of sorption to Fe minerals in increasing
437 the stability of relatively reactive labile compounds.

438

439 **Fig. 6**

440

441 Nitrogen (N)-containing functional groups are potentially important for the association
442 between OC and Fe oxides, although the concentrations of N are much lower than C (Yang et al.,
443 2012; Barber et al., 2014). The bulk soil contained 0.05-0.45 % N, while the non-Fe-bound
444 component (i.e. the residual solid after DCB extraction) contained 0.06-0.32 % N.
445 Concentrations of Fe-bound N, calculated by difference, ranged up to 0.13 %. However, it is
446 important to note that this number is based without a calibration for labile N that may be
447 removed by the dithionite-free DCB extraction (data not available). There were significant
448 correlations between C and N concentrations for both bulk soils ($r=0.847$, $p<0.001$:
449 Supplementary Material, Fig. S10) and the non-Fe-bound residual components ($r=0.858$,
450 $p<0.001$: Supplementary Material, Fig. S10), with molar C/N ratios of 14.2 ± 2.6 and 13.7 ± 2.3 for
451 bulk and non-Fe-bound OC, respectively. These C/N values are essentially identical to a
452 previously observed molar C/N ratio = 14.3 for a large set of world-wide soils samples
453 (Cleveland et al., 2007), and a molar C/N ratio = 14.4 for OC-rich samples in China (Tian et al.,
454 2010). This result suggests that C/N ratios for Fe-bound OC did not differ from that of non-Fe-
455 bound OC, assuming that the labile carbon did not have a substantially different C/N ratio.

456 Therefore, in contrast to the ^{13}C enrichment observed for Fe-bound OC, the interactions with Fe
457 minerals did not affect the C/N ratio substantially.

458

459 **4. Conclusion**

460 Overall, this study provided a comprehensive investigation into the amount and characteristics of
461 Fe-bound OC in forest soils as well as the impact of soil physicochemical properties on Fe-
462 bound OC. On average, Fe-bound OC contributed to 37.8% of TOC in forest soils, composing an
463 important component of C cycles in terrestrial ecosystem. The OC:Fe molar ratios in the forest
464 soils studied ranged from 0.56 to 17.7, indicating the importance of both sorptive and
465 incorporative interactions between Fe and OC. $f_{\text{Fe-OC}}$ increased with latitude, and reached the
466 peak value for soils with an annual mean temperature of 6.6°C , as a result of the temperature
467 dependence of Fe mineral phase and OC transformation. Combined studies of FTIR, NEXAFS,
468 and ^{13}C analysis revealed that Fe-bound OC was less aliphatic, more carboxylic, and more
469 enriched in ^{13}C , compared to non-Fe-bound OC. Assuming Fe-bound OC is relatively stable, Fe
470 oxides serve as a storage reservoir on decadal time scales for hydrophilic and carboxylic OC,
471 which would be otherwise relatively more available for microbial degradation.

472

473 **Acknowledgements**

474 This research was supported by DOE grant DE-SC0014275 and University of Nevada-Reno
475 Start-up Fund. NEXAF research described in this paper was performed at the Canadian Light
476 Source, which is supported by CFI, NSERC, the University of Saskatchewan, the Government of
477 Saskatchewan, WED Canada, NRC Canada, and CIHR. Sample collection was supported by a
478 former EPA Science-To-Achieve-Results (STAR) grant R833378. We also acknowledge the
479 helpful comments from the editor and reviewers during the stage of quick reports.

480

481 **References**

482 Adhikari, D. and Yang, Y.: Selective stabilization of aliphatic organic carbon by iron oxide, Sci. Rep., 5,
483 2015.

- 484 Adhikari, D., Poulson, S. R., Sumaila, S., Dynes, J. J., McBeth, J. M., and Yang, Y.: Asynchronous
485 reductive release of iron and organic carbon from hematite–humic acid complexes, *Chem. Geol.*, 430, 13-
486 20, 2016.
- 487 Amelung, W., Flach, K. W., and Zech, W.: Climatic effects on soil organic matter composition in the
488 great plains, *Soil Sci. Soc. Am. J.*, 61, 115-123, 1997.
- 489 Amundson, R.: The carbon budget in soils, *Annual Review of Earth and Planetary Sciences*, 29, 535-562,
490 2001.
- 491 Axe, K. and Persson, P.: Time-dependent surface speciation of oxalate at the water-boehmite (gamma-
492 AlOOH) interface: implications for dissolution, *Geochim. Cosmochim. Ac.*, 65, 4481-4492, 2001.
- 493 Baldock, J. A. and Skjemstad, J. O.: Role of the soil matrix and minerals in protecting natural organic
494 materials against biological attack, *Org. Geochem.*, 31, 697-710, 2000.
- 495 Barber, A., Lalonde, K., Mucci, A., & Gélinas, Y.: The role of iron in the diagenesis of organic carbon
496 and nitrogen in sediments: A long-term incubation experiment. *Mar. Chem.*, 162, 1-9, 2014.
- 497 Bar-Even, A., Flamholz, A., Noor, E., and Milo, R.: Rethinking glycolysis: on the biochemical logic of
498 metabolic pathways, *Nat. Chem. Biol.*, 8, 509-517, 2012.
- 499 Batjes, N. H.: Documentation to ISRIC-WISE global data set of derived soil properties on a ½° by ½°
500 grid (Version 1.0), International Soil Reference and Information Centre, Wageningen, The Netherlands,
501 1996.
- 502 Calderon, F. J., Reeves, J. B., III, Collins, H. P., and Paul, E. A.: Chemical differences in soil organic
503 matter fractions determined by diffuse-reflectance mid-infrared spectroscopy, *Soil Sci. Soc. Am. J.*, 75,
504 568-579, 2011.
- 505 Chorover, J. and Amistadi, M. K.: Reaction of forest floor organic matter at goethite, birnessite and
506 smectite surfaces, *Geochim. Cosmochim. Ac.*, 65, 95-109, 2001.
- 507 Cleveland, C. C. and Liptzin, D.: C : N : P stoichiometry in soil: is there a "Redfield ratio" for the
508 microbial biomass?, *Biogeochemistry*, 85, 235-252, 2007.
- 509 Conant, R. T., Ryan, M. G., Agren, G. I., Birge, H. E., Davidson, E. A., Eliasson, P. E., Evans, S. E., Frey,
510 S. D., Giardina, C. P., Hopkins, F. M., Hyvonen, R., Kirschbaum, M. U. F., Lavalley, J. M., Leifeld, J.,
511 Parton, W. J., Steinweg, J. M., Wallenstein, M. D., Wetterstedt, J. A. M., and Bradford, M. A.:
512 Temperature and soil organic matter decomposition rates - synthesis of current knowledge and a way
513 forward, *Glob. Change Biol.*, 17, 3392-3404, 2011.
- 514 Cornell, R. M., Giovanoli, R., and Schindler, P. W.: Effect of silicate species on the transformation of
515 ferrihydrite into goethite and hematite in alkaline media, *Clay. Clay Miner.*, 35, 21-28, 1987.
- 516 Davidson, E. A. and Janssens, I. A.: Temperature sensitivity of soil carbon decomposition and feedbacks
517 to climate change, *Nature*, 440, 165-173, 2006.
- 518 Eswaran, H., Reich, P. F., Kimble, J. M., Beinroth, F. H., Padmanabhan, E., and Moncharoen, P.: *Global
519 Climate Change and Pedogenic Carbonates*. Lal, R. (Ed.), Lewis Publishers, Boca Raton, FL. USA, 1999.

520 Eusterhues, K., Hadrich, A., Neidhardt, J., Kusel, K., Keller, T. F., Jandt, K. D., and Totsche, K. U.:
521 Reduction of ferrihydrite with adsorbed and coprecipitated organic matter: microbial reduction by
522 *Geobacter bremensis* vs. abiotic reduction by Na-dithionite, *Biogeosciences*, 11, 4953-4966, 2014.

523 Eusterhues, K., Rumpel, C., and Kogel-Knabner, I.: Organo-mineral associations in sandy acid forest
524 soils: importance of specific surface area, iron oxides and micropores, *Eur. J. Soil Sci.*, 56, 753-763, 2005.

525 Gillespie, A. W., Phillips, C. L., Dynes, J. J., Chevrier, D., Regier, T. Z., and Peak, D.: Advances in using
526 soft X-ray spectroscopy for measurement of soil biogeochemical processes, *Adv. Agron.*, 133, 1-32, 2015.

527 Glaser, B.: Compound-specific stable-isotope (δ C-13) analysis in soil science, *J. Plant Nutr. Soil Sci.*,
528 168, 633-648, 2005.

529 Gnanaprakash, G., Mahadevan, S., Jayakumar, T., Kalyanasundaram, P., Philip, J., and Raj, B.: Effect of
530 initial pH and temperature of iron salt solutions on formation of magnetite nanoparticles, *Mater. Chem.*
531 *Phys.*, 103, 168-175, 2007.

532 Gu, B. H., Schmitt, J., Chen, Z., Liang, L. Y., and McCarthy, J. F.: Adsorption and desorption of different
533 organic-matter fractions on iron-oxide, *Geochim. Cosmochim. Ac.*, 59, 219-229, 1995.

534 Guggenberger, G. and Kaiser, K.: Dissolved organic matter in soil: challenging the paradigm of sorptive
535 preservation, *Geoderma*, 113, 293-310, 2003.

536 Harsh, J. B., Chorover, J., Nizeyimana, E.: Allophane and imogolite. Chap. 9. In: *Soil Mineralogy with*
537 *environmental applications*, Dixon, J. B., Schulze, D. G.: (Ed.), Book Series SSSA No. 7, Madison, WI.,
538 2002.

539 Johnson, D. W., and Curtis, P. S.: Effects of forest management on soil C and N storage: meta analysis,
540 *Forest Ecol. Manag.*, 140, 227-238, 2001.

541 Kaiser, K. and Guggenberger, G.: Sorptive stabilization of organic matter by microporous goethite:
542 sorption into small pores vs. surface complexation, *Eur. J. Soil Sci.*, 58, 45-59, 2007.

543 Kalbitz, K., Schwesig, D., Rethemeyer, J., and Matzner, E.: Stabilization of dissolved organic matter by
544 sorption to the mineral soil, *Soil Biol. Biochem.*, 37, 1319-1331, 2005.

545 Kalra, Y. P., Agrawal, H. P., Allen, E., Ashworth, J., Audesse, P., Case, V. W., Collins, D., Combs, S. M.,
546 Dawson, C., Denning, J., Donohue, S. J., Douglas, B., Drought, B. G., Flock, M. A., Friedericks, J. B.,
547 Gascho, G. J., Gerstl, Z., Hodgins, L., Hopkins, B., Horneck, D., Isaac, R. A., Kelly, P. M., Konwicky, J.,
548 Kovar, J., Kowalenko, G., Lutwick, G., Miller, R. O., Munter, R., Murchison, I., Neary, A., Neumann, R.,
549 Neville, M., Nolan, C. B., Olive, R., Pask, W., Pastorek, L., Peck, T. R., Peel, T., Ramakers, J., Reid, W.
550 S., Rodd, V., Schultz, R., Simard, R., Singh, R. S., Sorrels, J., Sullivan, M., Tran, S., Trenholm, D., Trush,
551 J., Tucker, M. R., Turcotte, E., Vanniekerc, A., Vijan, P. N., Villanueva, J., Wang, C., Warneke, D. D.,
552 Watson, M. E., Wikoff, L., and Yeung, P.: Determination of pH of soils by different methods -
553 collaborative study, *J. AOAC Int.*, 78, 310-324, 1995.

554 Krull, E. S., Baldock, J. A., and Skjemstad, J. O.: Importance of mechanisms and processes of the
555 stabilization of soil organic matter for modelling carbon turnover, *Funct. Plant Biol.*, 30, 207-222, 2003.

556 Lalonde, K., Mucci, A., Ouellet, A., and Gélinas, Y.: Preservation of organic matter in sediments
557 promoted by iron, *Nature*, 483, 198-200, 2012.

558 Lehmann, J., Solomon, D., Kinyangi, J., Dathe, L., Wirick, S., and Jacobsen, C.: Spatial complexity of
559 soil organic matter forms at nanometer scales, *Nature Geosci.*, 1, 238-242, 2008.

560 Madejova, J.: FTIR techniques in clay mineral studies, *Vib. Spectrosc.*, 31, 1-10, 2003.

561 Mayer, L. M., Schick, L. L., Hardy, K. R., Wagai, R., and McCarthy, J.: Organic matter in small
562 mesopores in sediments and soils, *Geochim. Cosmochim. Ac.*, 68, 3863-3872, 2004.

563 Mayhew, S. G.: The redox potential of dithionite and SO^{-2} from equilibrium reactions with flavodoxins,
564 methyl viologen and hydrogen plus hydrogenase, *Eur. J. Biochem.*, 85, 535-547, 1978.

565 Mehra, O. P., and Jackson, M. L.: Iron oxide removal from soils and clays by a dithionite-citrate system
566 buffered with sodium bicarbonate, In *National Conference on Clay. Clay miner.*, 7, 317-327, 1960.

567 Obrist, D.: Mercury distribution across 14 U.S. forests. part II: patterns of methyl mercury concentrations
568 and areal mass of total and methyl mercury, *Environ. Sci. Technol.*, 46, 5921-5930, 2012.

569 Obrist, D., Johnson, D. W., Lindberg, S. E., Luo, Y., Hararuk, O., Bracho, R., Battles, J. J., Dail, D. B.,
570 Edmonds, R. L., Monson, R. K., Ollinger, S. V., Pallardy, S. G., Pregitzer, K. S., and Todd, D. E.:
571 Mercury distribution across 14 US forests. part I: spatial patterns of concentrations in biomass, litter, and
572 soils, *Environ. Sci. Technol.*, 45, 3974-3981, 2011.

573 Obrist, D., Zielinska, B., and Perlinger, J. A.: Accumulation of polycyclic aromatic hydrocarbons (PAHs)
574 and oxygenated PAHs (OPAHs) in organic and mineral soil horizons from four US remote forests,
575 *Chemosphere*, 134, 98-105, 2015.

576 Parikh, S. J., Goynes, K. W., Margenot, A. J., Mukome, F. N. D., and Calderon, F. J.: Soil Chemical
577 Insights Provided through Vibrational Spectroscopy, *Adv. Agron.*, 126, 1-148, 2014.

578 Percival, H. J., Parfitt, R. L., and Scott, N. A.: Factors controlling soil carbon levels in New Zealand
579 grasslands: Is clay content important?, *Soil Sci. Soc. Am. J.*, 64, 1623-1630, 2000.

580 Reeves, J. B., III: Mid-infrared spectral interpretation of soils: Is it practical or accurate?, *Geoderma*, 189,
581 508-513, 2012.

582 Regier, T., Krochak, J., Sham, T. K., Hu, Y. F., Thompson, J., and Blyth, R. I. R.: Performance and
583 capabilities of the Canadian Dragon: the SGM beamline at the Canadian Light Source, *Nuclear
584 Instruments & Methods in Physics Research Section a-Accelerators Spectrometers Detectors and
585 Associated Equipment*, 582, 93-95, 2007.

586 Riedel, T., Iden, S., Geilich, J., Wiedner, K., Durner, W., and Biester, H.: Changes in the molecular
587 composition of organic matter leached from an agricultural topsoil following addition of biomass-derived
588 black carbon (biochar), *Org. Geochem.*, 69, 52-60, 2014.

589 Riedel, T., and Weber, T. K.: The chemical potential of water in soils and sediments, *Soil Sci. Soc. Am. J.*,
590 80, 79-83, 2016.

591 Riley, W. J., Maggi, F., Kleber, M., Torn, M. S., Tang, J. Y., Dwivedi, D., and Guerry, N.: Long
592 residence times of rapidly decomposable soil organic matter: application of a multi-phase, multi-
593 component, and vertically resolved model (BAMS1) to soil carbon dynamics, *Geoscientific Model
594 Development*, 7, 1335-1355, 2014.

595 Scharlemann, J. P. W., Tanner, E. V. J., Hiederer, R., and Kapos, V.: Global soil carbon: understanding
596 and managing the largest terrestrial carbon pool, *Carbon Manag.*, 5, 81-91, 2014.

597 Schmidt, M. W. I., Torn, M. S., Abiven, S., Dittmar, T., Guggenberger, G., Janssens, I. A., Kleber, M.,
598 Kogel-Knabner, I., Lehmann, J., Manning, D. A. C., Nannipieri, P., Rasse, D. P., Weiner, S., and
599 Trumbore, S. E.: Persistence of soil organic matter as an ecosystem property, *Nature*, 478, 49-56, 2011.

600 Schumacher, M., Christl, I., Scheinost, A. C., Jacobsen, C., and Kretzschmar, R.: Chemical heterogeneity
601 of organic soil colloids investigated by scanning transmission X-ray microscopy and C-1s NEXAFS
602 microspectroscopy, *Environ. Sci. Technol.*, 39, 9094-9100, 2005.

603 Schwertmann, U. and Latham, M.: Properties of iron-oxides in some new caledonian oxisols, *Geoderma*,
604 39, 105-123, 1986.

605 Senesi, N., D'Orazio, V., and Ricca, G.: Humic acids in the first generation of EUROSOLS, *Geoderma*,
606 116, 325-344, 2003.

607 Simonetti, G., Francioso, O., Nardi, S., Berti, A., Brugnoli, E., Lugato, E., and Morari, F.:
608 Characterization of humic carbon in soil aggregates in a long-term experiment with manure and mineral
609 fertilization, *Soil Sci. Soc. Am. J.*, 76, 880-890, 2012.

610 Six, J., Callewaert, P., Lenders, S., De Gryze, S., Morris, S. J., Gregorich, E. G., Paul, E. A., and Paustian,
611 K.: Measuring and understanding carbon storage in afforested soils by physical fractionation, *Soil Sci.*
612 *Soc. Am. J.*, 66, 1981-1987, 2002.

613 Sollins, P., Homann, P., and Caldwell, B. A.: Stabilization and destabilization of soil organic matter:
614 Mechanisms and controls, *Geoderma*, 74, 65-105, 1996.

615 Solomon, D., Lehmann, J., Kinyangi, J., Liang, B. Q., and Schafer, T.: Carbon K-edge NEXAFS and
616 FTIR-ATR spectroscopic investigation of organic carbon speciation in soils, *Soil Sci. Soc. Am. J.*, 69,
617 107-119, 2005.

618 Staff, S. S.: Soil taxonomy: A basic system of soil classification for making and interpreting soil surveys.
619 2nd edition, Natural Resources Conservation Service. U.S. Department of Agriculture Handbook, 436,
620 1999.

621 Steffen, W., Noble, I., Canadell, J., Apps, M., Schulze, E. D., Jarvis, P. G., Baldocchi, D., Ciais, P.,
622 Cramer, W., Ehleringer, J., Farquhar, G., Field, C. B., Ghazi, A., Gifford, R., Heimann, M., Houghton, R.,
623 Kabat, P., Korner, C., Lambin, E., Linder, S., Mooney, H. A., Murdiyarso, D., Post, W. M., Prentice, I. C.,
624 Raupach, M. R., Schimel, D. S., Shvidenko, A., Valentini, R., and Terrestrial Carbon Working, G.: The
625 terrestrial carbon cycle: implications for the Kyoto Protocol, *Science*, 280, 1393-1394, 1998.

626 Tandy, S., Healey, J. R., Nason, M. A., Williamson, J. C., Jones, D. L., and Thain, S. C.: FT-IR as an
627 alternative method for measuring chemical properties during composting, *Bioresour. Technol.*, 101, 5431-
628 5436, 2010.

629 Tian, H., Chen, G., Zhang, C., Melillo, J. M., and Hall, C. A. S.: Pattern and variation of C:N:P ratios in
630 China's soils: a synthesis of observational data, *Biogeochemistry*, 98, 139-151, 2010.

631 Tipping, E., Rey-Castro, C., Bryan, S. E., and Hamilton-Taylor, J.: Al(III) and Fe(III) binding by humic
632 substances in freshwaters, and implications for trace metal speciation, *Geochim. Cosmochim. Ac.*, 66,
633 3211-3224, 2002.

634 Vogel, C., Mueller, C. W., Hoeschen, C., Buegger, F., Heister, K., Schulz, S., Schloter, M., and Koegel-
635 Knabner, I.: Submicron structures provide preferential spots for carbon and nitrogen sequestration in soils,
636 Nat. Commun., 5, 2014.

637 Wagai, R. and Mayer, L. M.: Sorptive stabilization of organic matter in soils by hydrous iron oxides,
638 Geochim. Cosmochim. Ac., 71, 25-35, 2007.

639 Wagai, R., Mayer, L. M., Kitayama, K., and Shirato, Y.: Association of organic matter with iron and
640 aluminum across a range of soils determined via selective dissolution techniques coupled with dissolved
641 nitrogen analysis, Biogeochemistry, 112, 95-109, 2013.

642 Wang, X. C., Druffel, E. R. M., Griffin, S., Lee, C., and Kashgarian, M.: Radiocarbon studies of organic
643 compound classes in plankton and sediment of the northeastern Pacific Ocean, Geochim. Cosmochim.
644 Ac., 62, 1365-1378, 1998.

645 Werner, R. A., Bruch, B. A., and Brand, W. A.: ConFlo III - An interface for high precision delta(13)C
646 and delta(15)N analysis with an extended dynamic range, Rapid. Commun. Mass Sp., 13, 1237-1241,
647 1999.

648 White, A. F., and Blum, A. E.: Effects of climate on chemical-weathering in watersheds, Geochim.
649 Cosmochim. Ac., 59, 1729-1747, 1995.

650 Wilson, B. T., Woodall, C.W., and Griffith, D.M.: Imputing forest carbon stock estimates from inventory
651 plots to a nationally continuous coverage, Carbon Balance and Manag., 8, 2013.

652 Yang, W. H., Weber, K. A., and Silver, W. L.: Nitrogen loss from soil through anaerobic ammonium
653 oxidation coupled to iron reduction. Nature Geosci., 5, 538-541, 2012.

654 Zelles, L., Bai, Q. Y., Beck, T., and Beese, F.: Signature fatty acids in phospholipids and
655 lipopolysaccharides as indicators of microbial biomass and community structure in agricultural soils, Soil
656 Biol. and Biochem., 24, 317-323, 1992.

657 Zhao, J. M., Huggins, F. E., Feng, Z., and Huffman, G. P.: Ferrihydrite-surface-structure and its effects on
658 phase-transformation, Clay. Clay Miner., 42, 737-746, 1994.

659

660

661

662

663

664

665

666

667

668

669

670

671 **Figure Captions**

672 **Figure 1.** Concentrations of total carbon (TC), total organic carbon (TOC) and Fe-bound OC in
673 14 forest soils across the United States. TC, TOC, and Fe-bound OC contents are generally
674 higher in soils with higher latitude (also shown in Figure 3). Duplicate measurements were
675 conducted for each of two plots in every forest site. Error bars represent standard deviation of
676 measurements of four replicates for each forest site.

677 **Figure 2.** Concentration of reactive Fe and OC:Fe molar ratio in the U.S. forest soils.

678 **Figure 3.** Relationships between TOC, concentration of Fe-bound OC, $f_{\text{Fe-TOC}}$ and
679 ecogeographical parameters including latitude, elevation (asl), and temperature (annual mean).

680 **Figure 4.** Relationships between the fractions of iron-bound organic carbon (uncalibrated for
681 loss of labile OC) and labile organic carbon and soil texture (i.e., fractions of sand, silt, and clay
682 in forest soils). Values of Pearson correlation coefficients (r) and significance levels were given.

683 **Figure 5.** Attenuated total reflectance-Fourier transform infrared spectroscopy (ATR-FTIR)
684 analysis for representative forest soils before (black line) and after Fe extraction (red line). All
685 the spectra are background-calibrated. Among the 14 forest soils sampled in this study, we used
686 five different forest soils, with $f_{\text{Fe-OC}}$ ranging 5.6-57.8%.

687 **Figure 6. A.** $\delta^{13}\text{C}$ of iron-bound and non-iron bound organic carbon for 14 U.S. forest sites. **B.**
688 Correlation between $\Delta^{13}\text{C}_{\text{FeOC-nonFeOC}}$ and molar ratio of OC:Fe.

689
690
691
692
693
694
695
696
697
698
699

Table 1 Information for the 14 forest sites studied (Obrist et al., 2011, 2012, 2015)

Forest ID	Abbr.	Location	Soil Order (US)	Soil Class ^a (FAO)	Climate Zone	LAT (°) ^b	LONG (°) ^c	Elevation (m asl)	Precip. ^d (mm y ⁻¹)	Temp ^e (°C)
Gainesville	GS	Gainesville, Florida	Spodosols	Podzols	Humid Subtropical	29.74	-82.22	50	1228	21.7
Oak Ridge	OR	Oak Ridge, Tennessee	Ultisols	Acrisols	Humid Subtropical	35.97	-84.28		1350	14.5
Ashland	AL	Ashland, Missouri	Alfisols	Luvisols & Greyzems	Humid Continental	38.73	-92.20	210	1023	13.9
Little Valley (post-fire)	LVF	Little Valley, Nevada	Entisols	Arenosols	Highland Climate	39.12	-119.93	2010	551	5.0
Little Valley	LV	Little Valley, Nevada	Entisols	Arenosols	Highland Climate	39.12	-119.93	2011	550	5.0
Marysville	MS	Marysville, California	Mollisols	Luvisols	Mediterranean climate	39.25	-121.28	386	775	16.9
Truckee (post-fire)	TKF	Truckee, California	Alfisols	Luvisols	Highland Climate	39.37	-120.1	1768	569	6.0
Truckee	TK	Truckee, California	Alfisols	Luvisols	Highland Climate	39.37	-120.1	1767	568	5.9
Niwot Ridge	NR	Niwot Ridge, Colorado	Alfisols	Cambisols	Highland Climate	40.03	-105.55	3050	800	1.3
Hart	HT	Hart, Michigan	Spodosols	Podzols	Humid Continental	43.67	-86.15	210	812	7.6
Bartlett	BL	Bartlett, New Hampshire	Spodosols	Podzols & Lithosols	Humid Continental	44.0	-71.29	272	1300	4.5
Howland	HL	Howland, Maine	Spodosols	Luvisols	Humid Continental	45.20	-68.74	60	1040	6.7
Thompson I	TSI	Ravensdale, Washington	Inceptisols	Cambisols	Highland Climate	47.38	-121.93	221	1141	9.8
Thompson II	TSII	Ravensdale, Washington	Inceptisols	Cambisols	Highland Climate	47.38	-121.93	220	1140	9.8

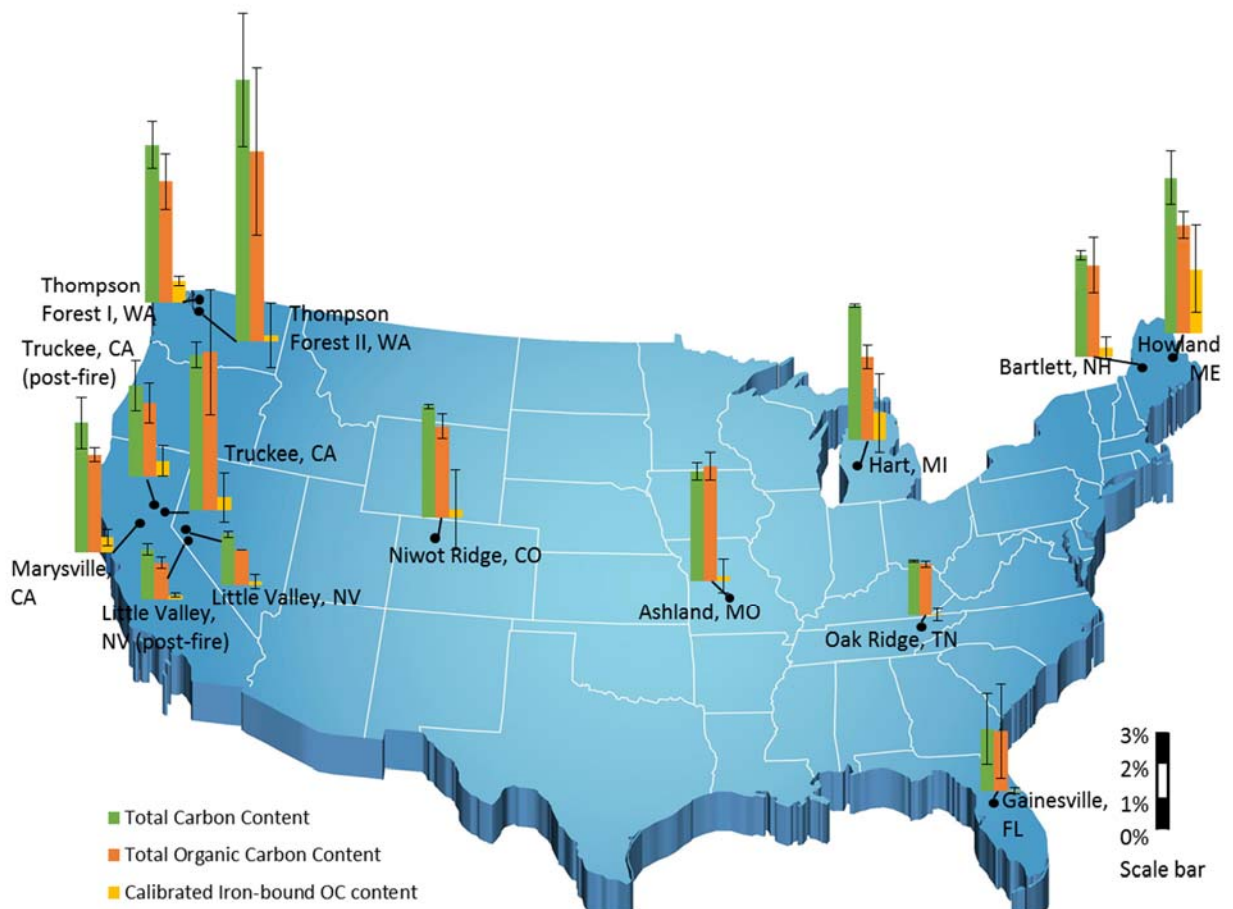
a: Food and Agriculture Organization; b latitude; c: longitude d: annual mean precipitation; e: annual mean temperature.

700

701

702

703



705

706

707 **Fig. 1**

708

709

710

711

712

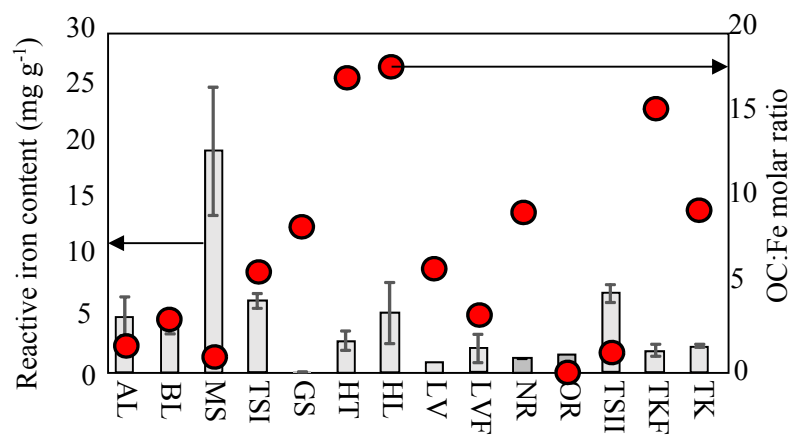
713

714

715

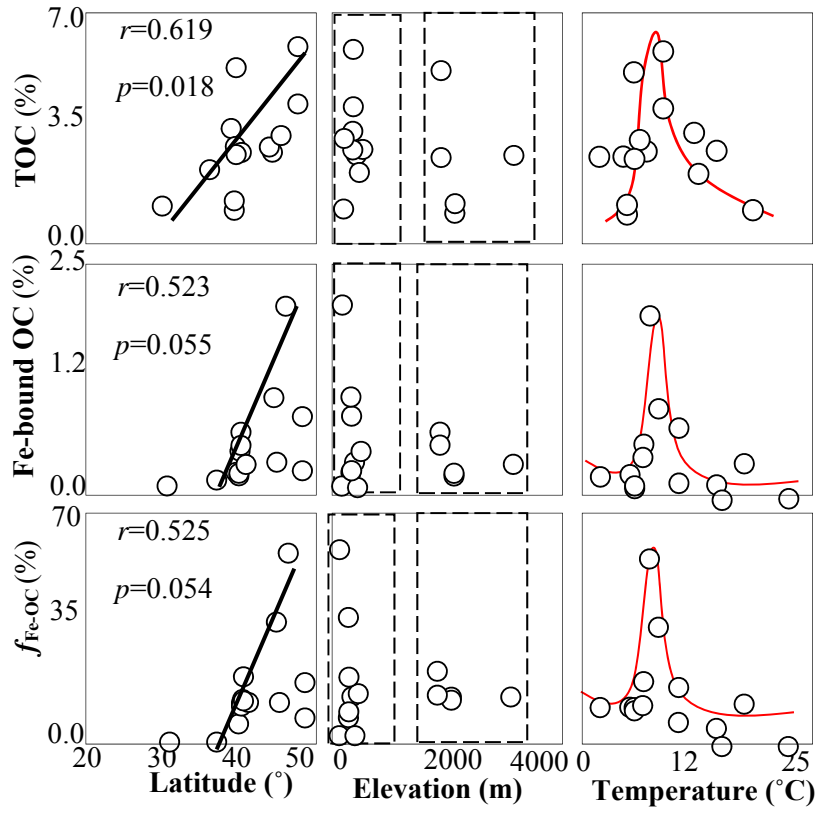
716

717



718 **Fig. 2**

719
 720
 721
 722
 723
 724
 725
 726
 727
 728
 729
 730
 731
 732
 733
 734
 735
 736
 737
 738
 739
 740



741 **Fig. 3**

742

743

744

745

746

747

748

749

750

751

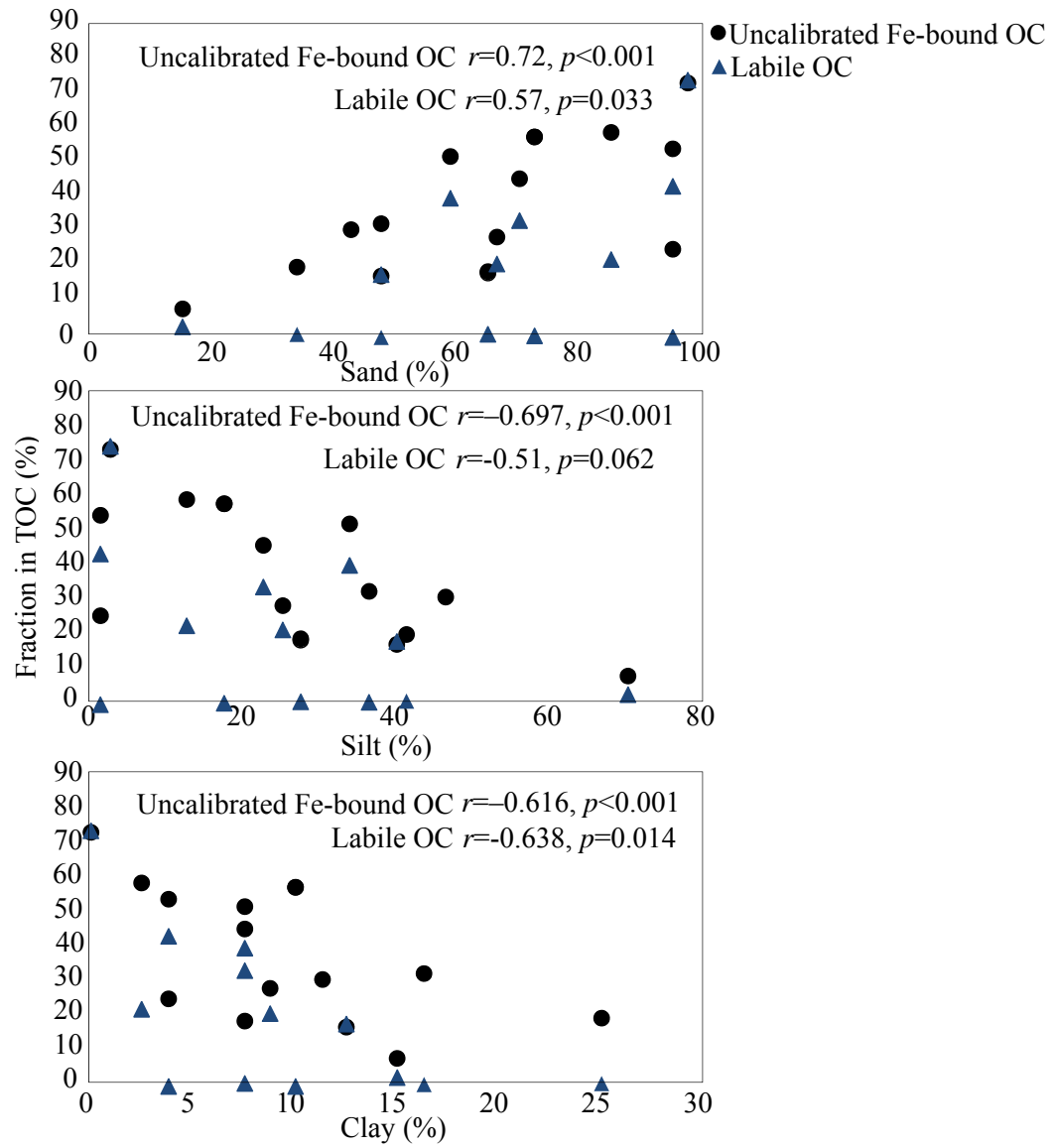
752

753

754

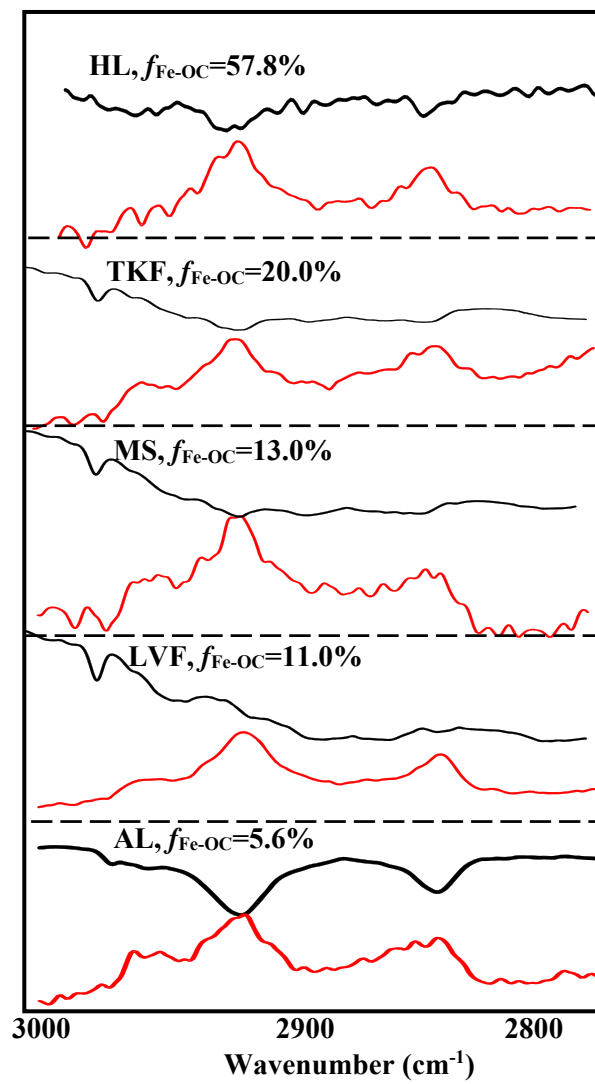
755

756



757
 758 **Fig. 4**

759
 760
 761
 762
 763
 764
 765
 766
 767



768 Fig. 5

769

770

771

772

773

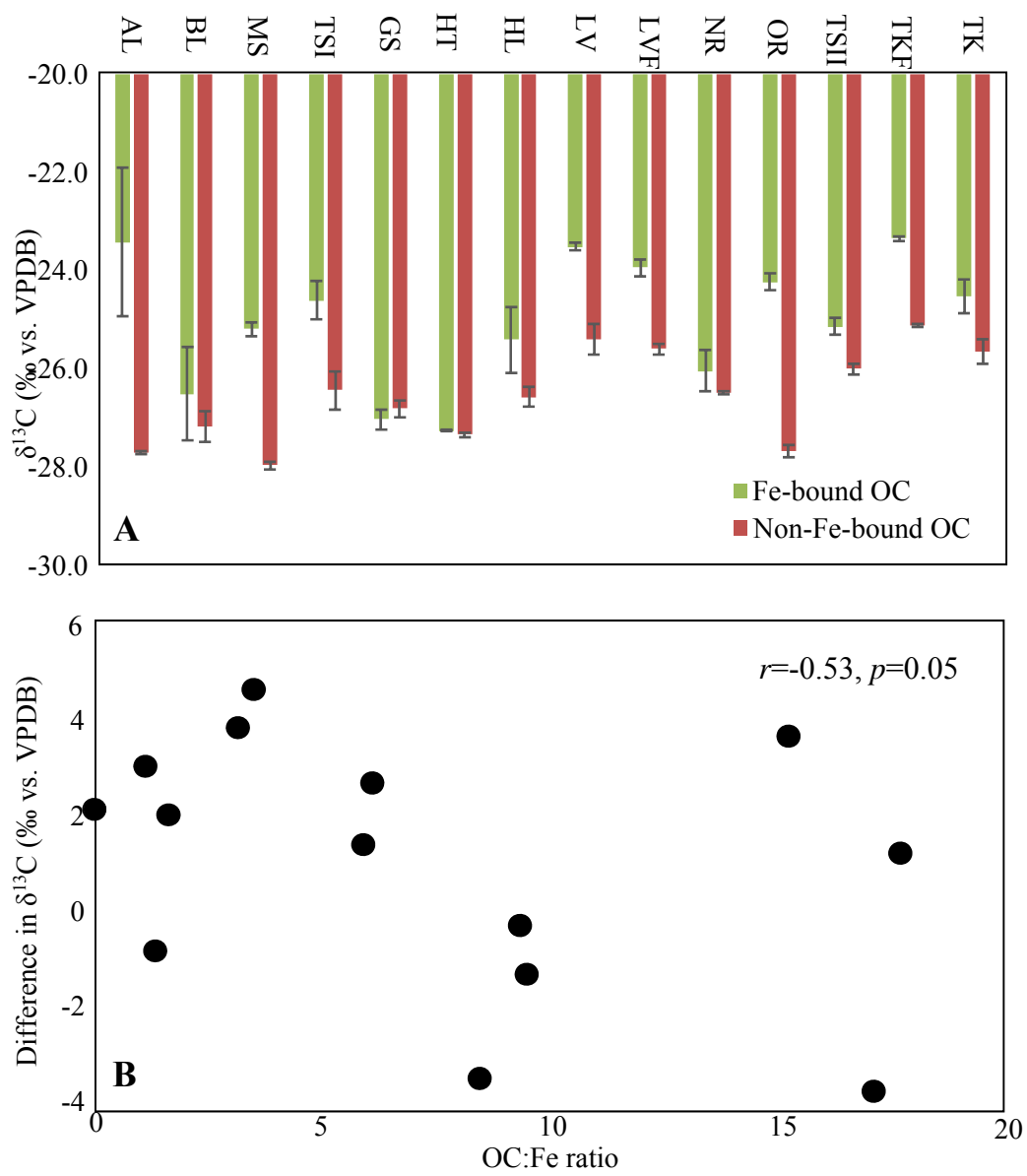
774

775

776

777

778



779 **Fig. 6**

780

781

782

783

784

785

786